Facial Plastic Surgery & Aesthetic Medicine
Volume 0, Number 0, 2023

DOI: 10.1089/fpsam.2022.0367

Facial Plastic Surgery & Aesthetic Medicine

Characterizing Olfactory Dysfunction in Patients with Unilateral Cleft Lip Nasal Deformities

Sarah M. Russel, MD, MPH,[1,2,†] Harry Chiang, MD,[2,†] John B. Finlay, MPhil,[2,3] Reanna Shah,[2] Jeffrey R. Marcus, MD,[4] David W. Jang, MD,[2] Ralph Abi Hachem, MD,[2] Bradley J. Goldstein, MD, PhD,[2,5] and Dennis Onyeka Frank-Ito, PhD[2,6,7,*]

Abstract

Background: Unilateral cleft lip nasal deformity (uCLND) is associated with olfactory dysfunction, but the underlying etiology remains poorly understood.

Objective: To investigate the etiology of uCLND-associated olfactory dysfunction using clinical, computational, and histologic assessments.

Methods: Inclusion criteria: uCLND patients >16 years undergoing septorhinoplasty. Exclusion criteria: prior septoplasty or rhinoplasty, pregnancy, sinusitis. Measured outcomes: patient-reported scores, rhinomanometry, smell identification and threshold tests, computational fluid dynamics (CFD) airflow simulations, and histologic analysis of olfactory epithelium.

Results: Five uCLND subjects were included: 18–23 years, three male and two female, four left-sided cleft and one right-sided cleft. All subjects reported moderate to severe nasal obstruction. Smell identification and threshold tests showed varying degrees of hyposmia. Nasal resistance was higher on the cleft side versus noncleft side measured by rhinomanometry (median 3.85 Pa-s/mL, interquartile range [IQR] = 21.96, versus 0.90 Pa-s/mL, IQR = 5.17) and CFD (median 1.04 Pa-s/mL, IQR = 0.94 vs. 0.11 Pa-s/mL, IQR = 0.12). Unilateral olfaction varied widely and was dependent on unilateral percentage olfactory airflow. Biopsies revealed intact olfactory neuroepithelium.

Conclusions: uCLND-associated olfactory dysfunction appears to be primarily conductive in etiology and highly susceptible to variations in nasal anatomy.

Clinical Trial Registration number: NCT04150783

[1]*Department of Otolaryngology/Head & Neck Surgery, University of North Carolina—Chapel Hill, Chapel Hill, North Carolina, USA.*
[2]*Department of Head and Neck Surgery & Communication Sciences, Duke University Medical Center, Durham, North Carolina, USA.*
[3]*Medical Scientist Training Program, Duke University School of Medicine, Durham, North Carolina, USA.*
[4]*Division of Plastic, Maxillofacial, and Oral Surgery, Department of Surgery, Duke University, Durham, North Carolina, USA.*
[5]*Department of Neurobiology, Duke University, Durham, North Carolina, USA.*
[6]*Department of Mechanical Engineering and Materials Science, Duke University, North Carolina, USA.*
[7]*Computational Biology & Bioinformatics PhD Program, Duke University, Durham, North Carolina, USA.*
[†]*These authors contributed equally to this work and are co-lead authors.*

*Address correspondence to: *Dennis Onyeka Frank-Ito, PhD, Department of Head and Neck Surgery & Communication Sciences, Duke University Medical Center, 40 Duke Medicine Circle, DUMC Box 3805, Durham, NC 27710, USA,* Email: dennis.frank@duke.edu

KEY POINTS

Question: Why do patients with unilateral cleft lip nasal deformities (uCLND) have decreased sense of smell?

Findings: Preliminary findings suggest that abnormalities in the nasal anatomy due to uCLND affect the flow of air to the olfactory region, although the sensory receptors and olfactory mucosa in these patients appear to be intact.

Meaning: Impaired sense of smell in patients with uCLND is likely due to insufficient flow of odorant-laden air to the olfactory region.

Introduction

Cleft lip deformities are associated with multiple malformations, including septal deviation, nasal aperture narrowing, turbinate hypertrophy, and maxillary growth deficits.[1,2] Cleft lip nasal deformities, particularly those in unilateral cleft phenotypes (uCLND), limit nasal breathing and lead to many quality-of-life concerns found in non-cleft nasal airway obstruction.[2–7]

However, patients with uCLND often prioritize aesthetic outcomes at the expense of improved functional outcomes, leading to an emphasis on cosmesis over function.[8,9] Balancing aesthetics with functional outcomes remains a challenge for reconstructive surgeons treating uCLND.

Further, uCLND is associated with diminished olfaction and worsened quality-of-life, but the mechanism underlying this deficit is not well described.[10–12] Normal odor detection requires (1) olfactory epithelium, which lines the olfactory cleft along the superior nasal septum and medial vertical lamellae of superior turbinates, and (2) airflow to the olfactory cleft, to permit interaction of inspired odorants with olfactory sensory neurons.

Olfactory neuronal axons project Cranial Nerve I through the cribriform plate to synapse in the glomerular layer of olfactory bulbs. As uCLND results from interruption of embryological development, uCLND-associated olfactory dysfunction could theoretically result from the disruption of either the sensorineural or conductive olfactory pathway. Deformities associated with uCLND can alter airflow to the olfactory cleft; however, developmental conditions resulting in cleft deformities could also disrupt the development of peripheral olfactory structures.

Therefore, contributions of conductive versus sensorineural etiologies remain unclear. Untreated smell loss is strongly linked to cognitive decline and depression[13–18]; hence, uCLND-associated olfactory dysfunction should not be neglected. Understanding the etiology of uCLND-associated olfactory dysfunction is key to determining how to improve smell in these patients.[10,11]

Among patients undergoing septorhinoplasty for uCLND, this prospective cohort study aimed at characterizing uCLND-associated olfactory dysfunction using olfactory assessments, computational fluid dynamics (CFD) modeling of nasal airflow, and histological analysis of olfactory epithelium.

Methods

Study subjects

This study, approved by the Duke University Health System Institutional Review Board, recruited six subjects with a clinical diagnosis of uCLND who elected to undergo septorhinoplasty. Eligible subjects were patients at least 16 years old and provided written informed consent. Exclusion criteria included (1) prior septoplasty or rhinoplasty, (2) active pregnancy, (3) inability to comply with study procedures, and (4) objective evidence of sinusitis on imaging.

Nasal Obstruction Symptom Evaluation (NOSE) and Standardized Cosmesis and Health Nasal Outcomes Survey (SCHNOS) questionnaires were collected for all participants.[19,20] Anterior rhinomanometry was performed to measure nasal airflow and resistance using the NR6 Clinical/Research Rhinomanometer (GM Instruments Ltd., Kilwinning, Scotland, United Kingdom); measurements were performed with the standard (75 Pa) technique. All data were gathered at patients' preoperative clinic visits.

Nasal airway reconstruction and CFD simulations

Preoperative cone beam computed tomography scans from each subject were read into imaging analysis software Avizo 3D 2021.1 (Thermo Fisher Scientific, Waltham, MA) to reconstruct three-dimensional models of their nasal airways. These models were segmented using Hounsfield unit thresholds -1024 to -300 HU with manual editing as needed, similar to previous models.[21–26]

To specify direction of inspiratory airflow in the nasal cavity, reconstructed nasal cavity models were imported into ICEM-CFD™ 2021 R1 (ANSYS, Canonsburg, PA) for creation of a box-like covering over the external nose to represent inlet for ambient air to flow into the nasal cavity. Further, reconstructed nasal cavity models were delineated to specify different anatomical regions: left/right nasal airspace, left/right olfactory airspace, and nasopharynx.

The olfactory airspace was defined from a coronal plane at the most anterior aspect of the middle turbinate to the anterior wall of the sphenoid sinus, and the inferior plane was created 10 mm below the cribriform plate.[27–30] Volume and surface area of each patient's unilateral nasal and olfactory airspace were calculated.

Each patient-specific nasal cavity model was imported into Fluent™ Meshing 2021 R1 (ANSYS), where ~ 4 million hybrid polyhedral-prismatic mesh elements

were created. Mesh quality analysis was used to smooth mesh elements with poor aspect ratio to prevent distorted elements from affecting accuracy of airflow simulations. Next, Fluent Solution 2021 R1 was used to simulate steady state, laminar inspiratory airflow in nasal passages at 15 L/min to mimic physiological resting respiration.[31–33]

The following boundary conditions were specified: a ''mass flow outlet'' condition at the outlet to target 0.000301 kg/s (15 L/min); atmospheric conditions at the inlet with zero-gauge pressure; and a stationary nasal cavity wall with no-slip conditions. Nasal airflow was calculated in all airspaces both throughout nasal cavities and at local, predefined sites, such as the olfactory cleft. Similarly, nasal resistance was calculated as $\Delta P/Q$ (Pa-s/mL), where ΔP represents pressure drop from nostrils to choana, and Q is volumetric flow rate. The percentage of unilateral olfactory flow relative to total unilateral nasal flow (percentage olfactory flow [POF]) was also calculated.

Measures of olfactory function

Two psychophysical tests of olfactory function were performed at patients' preoperative visits: University of Pennsylvania Smell Identification Test (SIT) (Sensonics, Inc., Haddon Heights, NJ) was used to assess odor identification, and Snap & Sniff® Threshold Test (SSTT) was used to determine odor threshold.[34–36] SIT was performed bilaterally, and SSTT was conducted unilaterally on each side.

Olfactory histological analysis—tissue collection

All tissue specimens were collected during standard surgical treatment at the Duke Cleft & Craniofacial Center, as previously described.[37] Briefly, olfactory epithelium biopsies were performed by otolaryngologists during septorhinoplasty. Once the olfactory cleft region was visualized endoscopically, the superior olfactory strip of septal mucosa was incised and elevated. Through-cutting, forceps were used to excise a small portion of mucosa with care to preserve integrity of olfactory tissue. Tissue was immediately placed in Hibernate-E Medium (A1247601; Thermo Fisher) +10% fetal bovine serum on ice and transferred to a lab. Biopsy was taken from the unilateral side that was more accessible to reach the olfactory cleft.

Olfactory histological analysis—tissue processing

Tissue was washed in PBS and fixed in 4% paraformaldehyde in PBS (Sigma-Aldrich, St. Louis, MO) for 3–6 hours at room temperature. After fixation, tissue was serially washed in PBS and incubated in 30% sucrose, 250 mM EDTA, and PBS on a rocker at 4°C for at least 5 days. Tissue was then placed in OCT (VWR, Radnor, PA) and flash frozen with liquid nitrogen. Ten micrometers sections were prepared using a CryoStar NX50 cryostat (Thermo Fisher), collected on glass slides (Superfrost plus; Thermo Fisher), and stored at −20°C.

Olfactory histological analysis—immunohistochemistry

Slides were rehydrated in PBS for 5 min. If antigen retrieval was required for the primary antibody (Ki-67, OMP), samples were further dehydrated/rehydrated in 75% ethanol for 1 min, 95% ethanol for 1 min, 100% ethanol for 1 min, 95% ethanol for 1 min, 75% ethanol for 1 min, and then PBS. Antigen retrieval was then performed by steaming slides in citrate-based antigen unmasking solution (Vector Laboratories, Newark, CA) for 40 min.

All tissue sections were blocked in buffer (5% normal donkey serum, 0.1% Triton-X-100, PBS) for 45 min at room temperature in a moist chamber. Samples were then incubated in primary antibody in a moist chamber either at 4°C overnight (Ki-67, OMP) or at room temperature for 1 hour (all other antibodies). Primary antibodies included: anti-Tubulin β3 (clone Tuj1, 1:500; BioLegend), anti-ERMN (PA5-58327, 1:100; Thermo Fisher), anti-SOX2 (No. 14-9811-82, 1:50; Invitrogen eBioscience), anti-OMP (sc-365818, 1:500; Santa Cruz), or anti-Ki-67 (ab15580, 1:250; Abcam).

All primary and secondary antibodies were diluted in blocking buffer. Slides were washed three times for 5 min each in PBS +0.3% Triton-X-100 and then incubated with species-specific fluorescent conjugated secondary antibodies (Jackson ImmunoResearch, West Grove, PA) for1 hour at room temperature in a moist chamber. Slides were again washed three times for 5 min each in PBS, stained with Hoecsht nuclear dye (1:1000; Thermo Fisher) for 3 min, and coverslipped with Vectashield (Vector Laboratories).

Results

Subject demographics and symptoms

Six patients with uCLND who were scheduled for septorhinoplasty were enrolled from April 2021 to June 2022. One patient was excluded due to extensive allergic fungal sinusitis diagnosed during clinical workup. Five patients, aged 18–23 years, were included—three males and two females. Consistent with previous findings, the cleft was more frequently left-sided (in 4/5 patients).[38] All patients demonstrated at least a moderate level of nasal obstruction with median (interquartile range [IQR]) NOSE and SCHNOS-Obstruction (SCHNOS-O) scores of 65 (IQR = 33.75) and 60 (IQR = 10), respectively (Table 1). For reference, NOSE scores are graded mild (5–25), moderate (30–50), severe (55–75), and extreme (80–100) obstruction, whereas SCHNOS-O scores are graded mild (0–40), moderate (45–75), and severe (75–100) obstruction.[39,40]

Table 1. Subject demographics, clinical nasal obstruction scores, anatomic measurements, olfactory scores and measurements, nasal resistance measurements, nasal and olfactory flow parameters, and nasal vestibule morphologies

Subject	*1*	*2*	*3*	*4*	*5*
Age	18	18	21	19	23
Sex	M	M	M	F	F
Cleft side	L	L	L	R	L
NOSE	45	65	45	90	75
SCHNOS-O	60	85	60	45	60
Cleft nasal volume (cm^3)	7.122	3.972	5.267	4.689	8.335
Noncleft nasal volume (cm^3)	7.196	11.468	13.898	8.193	10.703
Cleft olfactory volume (cm^3)	0.001	0.117	0.150	0.033	0.193
Noncleft olfactory volume (cm^3)	0.024	0.316	0.465	0.153	0.396
Cleft olfactory surface area (cm^2)	0.060	2.960	4.292	1.210	3.781
Noncleft olfactory surface area (cm^2)	0.879	5.664	7.807	3.395	6.722
Bilateral resistance rhinomanometry (Pa-s/mL)	0.59	10.35	0.88	0.65	0.91
Cleft resistance rhinomanometry (Pa-s/mL)	3.25	21.40	37.50	3.85	3.54
Noncleft resistance rhinomanometry (Pa-s/mL)	0.72	20.04	0.90	0.78	1.23
Bilateral resistance CFD (Pa-s/mL)	0.38	0.06	0.10	0.12	0.07
Cleft resistance CFD (Pa-s/mL)	1.04	1.73	1.26	0.53	0.18
Noncleft resistance CFD (Pa-s/mL)	0.39	0.06	0.11	0.15	0.11
SIT	20	29	35	31	29
Cleft SSTT (log vol/vol)	−3.25	−4.88	−5.88	−2.63	−5.88
Noncleft SSTT (log vol/vol)	−4.75	−4.88	−5.38	−5.25	−4.75
Cleft nasal flow (L/m)	0.98	0.03	1.27	3.43	5.88
Noncleft nasal flow (L/m)	14.00	14.97	13.73	11.57	9.12
Cleft maximum olfactory flow (L/m)	1.6E-03	2.7E-03	0.30	0.08	0.31
Noncleft maximum olfactory flow (L/m)	0.05	0.37	0.40	0.33	0.39
Cleft maximum percentage olfactory flow (%)	0.00	0.08	0.24	0.02	0.05
Noncleft maximum percentage olfactory flow (%)	0.00	0.02	0.03	0.03	0.04
Cleft nasal vestibule phenotype	N	N	S	N	S
Noncleft nasal vestibule phenotype	S	S	E	S	S

CFD, computational fluid dynamics; E, elongated; F, female; L, left; M, male; *N*, notched; NOSE, Nasal Obstruction Symptom Evaluation; OE, olfactory epithelium; R, right; RE, respiratory epithelium; S, standard; SCHNOS, Standardized Cosmesis and Health Nasal Outcomes Survey; SSTT, Snap & Sniff®® Threshold Test; U, unavailable; SIT, University of Pennsylvania smell identification test.

Nasal anatomy

Nasal cavity volume, olfactory airspace volume, and olfactory airspace surface area were smaller on the cleft side for all patients (Table 1). Median cleft nasal cavity volume was 5.267 cm^3 (IQR = 2.916) versus 10.703 cm^3 (IQR = 4.132) on the noncleft side (Table 1 and Fig. 1A). Median cleft olfactory airspace volume was 0.117 cm^3 (IQR = 0.136) versus 0.316 cm^3 (IQR = 0.293) on the noncleft side (Fig. 1A). Median cleft olfactory airspace surface area was 2.960 cm^2 (IQR = 2.986) versus 5.664 cm^2 (IQR = 4.227) on the noncleft side (Table 1).

Olfaction

Patients demonstrated varying degrees of olfactory impairment (median SIT score = 29, IQR = 5.25). Median SSTT unilateral olfactory scores were −4.88 log vol/vol (IQR = 2.78) on the cleft side and −4.88 log vol/vol (IQR = 0.53) on the noncleft side. More negative values represent lower concentrations of odorant required for odor detection and more sensitive olfactory thresholds (Table 1). For reference, the 50th-percentile SSTT is −5.44 log vol/vol, and −4.88 falls between the 30th (−4.63) and 40th (−5.00) percentiles.[41]

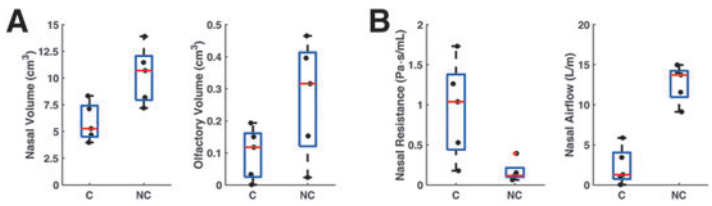

Fig. 1. Median nasal volume and olfactory volume were lower on the cleft side (C) than on the noncleft side (NC). In addition, nasal volumes and olfactory volumes were smaller on the cleft side than the noncleft side across all subjects **(A)**. Median nasal resistance was greater on the cleft side than on the noncleft side, and median nasal airflow was lower on the cleft side than on the noncleft side. In addition, nasal resistances were greater on the cleft side and nasal airflows were lower on the cleft side across all subjects **(B)**.

Notably, the cleft side was not consistently associated with a decreased olfaction despite smaller olfactory airspace volumes and greater nasal resistance—in Subject 2, cleft and noncleft olfactory thresholds were equal, and in Subjects 3 and 5, the cleft side threshold was lower than the noncleft side, demonstrating enhanced odor detection despite increased unilateral nasal resistance (Fig. 2).

Nasal resistance

Median bilateral nasal resistance from rhinomanometry and CFD analysis were 0.88 Pa-s/mL (IQR = 2.64) and 0.10 Pa-s/mL (IQR = 0.12), respectively (Table 1). These rhinomanometry measurements are in agreement with those in the literature for uCLND.[42] For all patients, unilateral nasal resistance was greater on the cleft side than the noncleft side. Median unilateral nasal resistance measured by rhinomanometry was 3.85 Pa-s/mL (IQR = 21.96) on the cleft side and 0.90 Pa-s/mL (IQR = 5.17) on the noncleft side. CFD-computed median unilateral resistance was 1.04 Pa-s/mL (IQR = 0.94) on the cleft side and 0.11 Pa-s/mL (IQR = 0.12) on the noncleft side (Table 1 and Fig. 1B).

Unilateral airflow

Unilateral nasal airflow rates were lower on the cleft side for all patients with median cleft-side flow of 1.268 L/m (IQR = 3.298) and noncleft flow of 13.728 L/m (IQR = 3.287) (Table 1 and Fig. 1B). Flow rates through the olfactory airspace were also lower on the cleft side for all subjects with median maximal flow of 0.085 L/m (IQR = 0.302) and noncleft-side maximal flow of 0.372 L/m (IQR = 0.136).

Contrary to universally lower flow rates on the cleft side, the percentage of unilateral olfactory flow relative to total unilateral nasal flow (POF) was higher on the cleft side for some patients. For Subjects 2, 3, and 5, POF was higher on the cleft side, and these reflected the patients with equal or better odor detection on the cleft side than the noncleft side (Fig. 2). Median POF was 5.21% (IQR = 10.11) on the cleft side and 2.83% (IQR = 1.29) on the noncleft side.

Airflow streamlines

The CFD-generated airflow streamlines were used to examine flow behavior. These streamlines demonstrated complex interactions between nasal anatomy and simulated airflow (Fig. 3 and Supplementary Fig. S1). In several patients, small variations in nasal vestibule morphology were associated with dramatic downstream effects on airflow, leading to discrepancies in POF (Table 1). Major anatomic contributors to altered airflow streamlines included different nasal vestibule phenotypes, which affects airflow at the anterior-superior airspace, and septal deviation, which caused airflow restriction and shunting of airflow around the septal spur.

Olfactory epithelium immunohistochemistry

Intraoperative biopsy in two patients yielded intact olfactory epithelium (Subjects 2 and 3), Subject 5 biopsy was unavailable, and biopsy captured in Subjects 1 and 4 was respiratory epithelium rather than olfactory

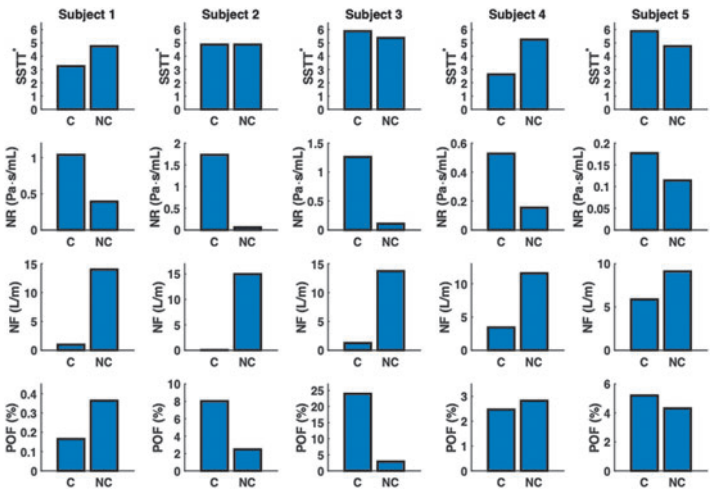

Fig. 2. SSTT, NR, NF, and POF for each subject. Despite greater nasal resistances and lower nasal flow rates on the cleft side across all subjects, olfaction measured by SSTT was not clearly correlated with cleft (C) versus noncleft side (NC). Rather, there was a greater association between POF and olfaction. Strikingly, in all subjects with equal or increased olfaction on the cleft side, the POF was also greater on the cleft side. *Of note, Snap & Sniff thresholds are presented as absolute values for ease of comparison with POF, where a higher absolute value indicates a lower odorant threshold or higher olfactory acuity. NF, nasal flow rates; NR, nasal resistances; POF, percentage olfactory flow; SSTT, Snap & Sniff® Threshold Test.

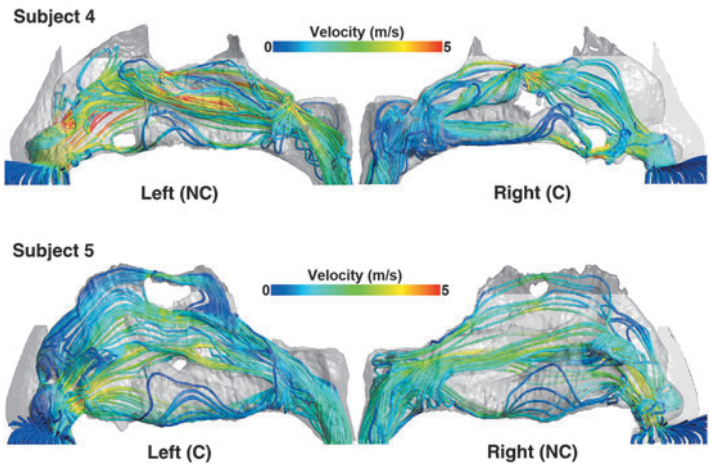

Fig. 3. Representative airflow streamlines for two subjects (top and bottom). Subject 4 (top) demonstrates an increased proportion of airflow streamlines entering the olfactory airspace (dark gray) on the noncleft side (top left) than the cleft side (top right), which is associated with a greater POF on the noncleft side than the cleft side. Accordingly, Subject 4's sense of smell is greater on the noncleft side than on the cleft side based on Snap & Sniff threshold testing. Subject 5 (bottom) demonstrates an increased proportion of airflow streamlines entering the olfactory airspace (dark gray) on the cleft side (bottom left) than the noncleft side (bottom right), which is associated with a greater POF on the cleft side than the noncleft side. Accordingly, Subject 5's sense of smell is greater on the cleft side than on the noncleft side based on Snap and Sniff threshold testing.

epithelium. Immunohistochemical staining of olfactory epithelium demonstrated healthy tissue architecture with positive staining of all markers for olfactory sensory neurons, support cells, and basal progenitor cells (Fig. 4; Subject 3).

TUJ1 and OMP markers showed evenly distributed immature and mature olfactory sensory neurons with thick axonal bundles extending into the lamina propria. Sustentacular cells as well as globose basal cells and horizontal basal cells also stained positively throughout the olfactory epithelium with ERMN, Ki-67, and SOX2, respectively (Fig. 4; Subject 3).

Discussion

Consistent with previous studies, the cleft side was associated with increased nasal resistance, smaller nasal airspace, and smaller olfactory volume.[23–25,43–45] In these patients with uCLND, the anatomic contributions leading to reduced cleft-side nasal volumes were multifactorial and included nasal alar phenotype, complex septal deviation, middle turbinate concha bullosa, and inferior turbinate hypertrophy. Although these deformities were not present among all subjects, each case involved multiple levels of obstruction throughout the airspace, which mirrored results from prior studies.[3–5,24,25,46,47]

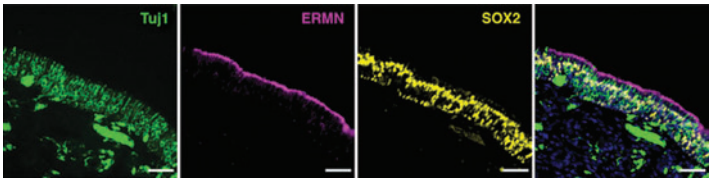

Fig. 4. Immunohistochemical staining of representative (Subject 3) olfactory epithelium demonstrating healthy tissue architecture with even distribution of both immature (Tuj1) and mature (OMP) olfactory sensory neurons. Likewise, sustentacular cells (ERMN), globose basal cells (Ki67), and horizontal basal cells (SOX2) also stain positively. Scale bars represent 50 μm.

In patients with uCLND, immunohistochemical staining of two olfactory mucosa biopsies (Subjects 2 and 3) was positive for all olfactory neuronal markers with similar cell distribution and density to that in the normosmic population. Of note, small biopsy sampling of olfactory tissue often fails to yield intact surface epithelium even in normosmics—patches of respiratory epithelium are commonly interspersed within olfactory areas, and sampling error may miss olfactory epithelium.[48,49] We consequently focused our analysis on successful biopsies from hyposmic cleft subjects, which was consistent with intact olfactory development. Preliminary data from this work suggest uCLND-associated olfactory changes may be primarily conductive in etiology.

Whereas nasal resistance and airflow were uniformly worse on the cleft side, olfactory threshold for odor detection did not demonstrate a clear association with either side. Rather, the unilateral olfactory threshold was more closely associated with POF (Fig. 2). Two conductive variables likely influence olfactory performance: nasal vestibule morphology and POF. In the ambient setting, air flows toward the side of least resistance at the level of the nasal vestibule; thus, a greater number of odorant molecules enter that airspace.

In the absence of septal perforation and retronasal olfaction, the total quantity of odorant molecules remains constant within the ipsilateral nasal cavity once airflow passes the nasal vestibule. However, the quantity of odorant molecules that reach the olfactory epithelium depends on their distribution across various regions of the unilateral nasal airway. Despite more odorant molecules on the noncleft side, lower nasal resistance in the inferior aspect of nasal airways can lead to shunting of airflow inferiorly away from the olfactory region, leading to the delivery of fewer odorant molecules and diminished odor detection.

Thus, POF, the proportion of airflow that reaches the olfactory cleft, appears to correlate better with olfaction than nasal resistance and airflow. Interactions among these parameters are illustrated through two scenarios. Scenario 1 (Fig. 2, Subjects 1 and 4, and Fig. 3, top) is characterized by increased cleft-side nasal resistance, diminished cleft-side nasal airflow, and diminished cleft-side POF compared with the noncleft side.

This correlates with decreased olfactory acuity on the cleft side compared with the noncleft side. Scenario 2 (Fig. 2, Subjects 2, 3, and 5; Fig. 3, bottom) is characterized by increased cleft-side nasal resistance, diminished cleft-side nasal airflow, yet increased cleft-side POF relative to the noncleft side. In this case, the cleft-side olfactory threshold is equal to or greater than the noncleft side.

Unilateral airflow analysis suggests that POF is dependent on not only locoregional anatomy but also unilateral nasal anatomy, particularly the nasal vestibule (Table 1). Certain nasal vestibule morphologies caused shunting of airflow inferiorly, with most airflow bypassing the olfactory region despite a widely patent olfactory airspace (Supplementary Fig. S1). As the initial entry point into the nasal cavity, the nasal vestibule profoundly affects subsequent airflow, including into the olfactory region.[21,27]

Ramprasad and Frank-Ito[50] described three distinct normal nasal vestibule morphology variations; ''Notched,'' ''Standard,'' and ''Elongated.'' The presence of a notch narrows the nasal vestibule airspace. These nasal vestibule morphological variations do not impact global airflow dynamics and resistance in healthy normal subjects but localized airflow, resistance, and transport of particulate matter, as well as odorant molecules in the nasal cavity were influence by nasal vestibule type.[21,27,50–53]

In one model, which placed virtual nasal polyps in varying locations, the greatest decrease in olfactory airflow occurred when polyps were located anterior to the olfactory region.[54] In a different study, virtual middle turbinectomy led to inconsistent changes in olfactory airflow; although olfactory airflow improved in most cases, one virtual middle turbinectomy caused turbulent airflow and shunting of airflow inferiorly below the olfactory region. Based on these findings, the interaction between nasal anatomy and olfactory airflow likely depends on multifactorial anatomical variations.[55]

Conclusion

Preliminary findings suggest that uCLND-associated olfactory dysfunction may be related to obstruction of airflow and odorants to the olfactory cleft rather than from sensorineural impairment. To our knowledge, this study is the first to explore pathophysiology of cleft-associated olfactory dysfunction. Airflow and odorant transport are highly dependent on variations in nasal anatomy, including nasal vestibule morphology, septal deviation, and more. The percentage of unilateral airflow to the olfactory airspace may be associated with olfactory function and smell threshold ability.

Acknowledgments

Special thanks are due to ANSYS, ANSYS Global Academic Program, and Dr. Paolo Maccarini (Duke University) for support and strategic donation.

Authors' Contributions

S.M.R.: Conceptualization, data curation, formal analysis, investigation, methodology, validation, visualization, writing—original draft, writing—review and editing. H.C.: Data curation, formal analysis, validation, visualization, writing—original draft, writing—review and editing. J.B.F.: Data curation, formal analysis, investigation, methodology, validation, visualization, writing—original draft, writing—review and editing. R.S.: Data curation,

formal analysis, investigation, methodology, validation, writing—review and editing. J.R.M.: Conceptualization, formal analysis, funding acquisition, investigation, methodology, project administration, resources, supervision, writing—review and editing. D.W.J.: Conceptualization, data curation, investigation, methodology, resources, writing—review and editing. R.A.H.: Conceptualization, data curation, investigation, methodology, resources, writing—review and editing. B.J.G.: Conceptualization, data curation, formal analysis, funding acquisition, investigation, methodology, project administration, resources, software, supervision, validation, visualization, writing—review and editing. D.O.F.-I.: Conceptualization, data curation, formal analysis, funding acquisition, investigation, methodology, project administration, resources, software, supervision, validation, visualization, writing—original draft, writing—review and editing. All co-authors have reviewed and approved the manuscript before submission.

Disclaimer

The content is solely the responsibility of the authors and does not necessarily represent the official views of the National Institutes of Health.

Author Disclosure Statement

D.W.J. and R.A.H. receive research funding from Amgen and GlaxoSmithKline; D.W.J. is a consultant for Medtronic; B.J.G. has consulted for Frequency Therapeutics and Rhino Therapeutics; the other authors have no disclosures.

Funding Information

National Institute of Dental & Craniofacial Research of the National Institutes of Health, Award Number R01 DE028554 and R01 DE028554-S1. This work was also funded in part from the NIH NIDCD grant supporting SMR (T32 DC005360).

Supplementary Material

Supplementary Figure S1

References

1. Hairfield WM, Warren DW, Hinton VA, Seaton DL. Inspiratory and expiratory effects of nasal breathing. *Cleft Palate J*. 1987;24(3):183–189.
2. Drettner B. The nasal airway and hearing in patients with cleft palate. *Acta Otolaryngol*. 1960;52(1–6):131–142.
3. Massie JP, Runyan CM, Stern MJ, et al. Nasal septal anatomy in skeletally mature patients with cleft lip and palate. *JAMA Facial Plast Surg*. 2016;18(5):347–353.
4. Fisher MD, Fisher DM, Marcus JR. Correction of the cleft nasal deformity: from infancy to maturity. *Clin Plast Surg*. 2014;41(2):283–299.
5. Starbuck JM, Friel MT, Ghoneima A, Flores RL, Tholpady S, Kula K. Nasal airway and septal variation in unilateral and bilateral cleft lip and palate. *Clin Anat*. 2014;27(7):999–1008.
6. Marcusson A, Akerlind I, Paulin G. Quality of life in adults with repaired complete cleft lip and palate. *Cleft Palate Craniofac J*. 2001;38(4):379–385.
7. Morén S, Mani M, Lundberg K, Holmström M. Nasal symptoms and clinical findings in adult patients treated for unilateral cleft lip and palate. *J Plast Surg Hand Surg*. 2013;47(5):383–389.
8. Noor SNFM, Musa S. Assessment of patients' level of satisfaction with cleft treatment using the Cleft Evaluation Profile. *Cleft Palate Craniofac J*. 2007;44(3):292–303.
9. Oosterkamp B, Dijkstra P, Remmelink H, et al. Satisfaction with treatment outcome in bilateral cleft lip and palate patients. *Int J Oral Maxillofac Surg*. 2007;36(10):890–895.
10. Grossmann N, Brin I, Aizenbud D, Sichel J-Y, Gross-Isseroff R, Steiner J. Nasal airflow and olfactory function after the repair of cleft palate (with and without cleft lip). *Oral Surg Oral Med Oral Pathol Oral Radiol Endod*. 2005;100(5):539–544.
11. May MA. *Olfactory Deficits in Cleft Lip and Palate*. Pittsburgh, PA: University of Pittsburgh; 2011.
12. Richman RA, Sheehe PR, McCanty T, et al. Olfactory deficits in boys with cleft palate. *Pediatrics*. 1988;82(6):840–844.
13. Graves AB, Bowen J, Rajaram L, et al. Impaired olfaction as a marker for cognitive decline: interaction with apolipoprotein E ε4 status. *Neurology*. 1999;53(7):1480.
14. Swan GE, Carmelli D. Impaired olfaction predicts cognitive decline in nondemented older adults. *Neuroepidemiology*. 2002;21(2):58–67.
15. Lafreniere D, Mann N. Anosmia: loss of smell in the elderly. *Otolaryngol Clin North Am*. 2009;42(1):123–131.
16. Mullol J, Alobid I, Mariño-Sánchez F, et al. Furthering the understanding of olfaction, prevalence of loss of smell and risk factors: a population-based survey (OLFACAT study). *BMJ Open*. 2012;2(6):e001256.
17. Doty RL. Epidemiology of smell and taste dysfunction. *Handb Clin Neurol*. 2019;164:3–13.
18. Doty RL. The mechanisms of smell loss after SARS-CoV-2 infection. *Lancet Neurol*. 2021;20(9):693–695.
19. Stewart MG, Smith TL, Weaver EM, et al. Outcomes after nasal septoplasty: results from the Nasal Obstruction Septoplasty Effectiveness (NOSE) study. *Otolaryngol Head Neck Surg*. 2004;130(3):283–290.
20. Moubayed SP, Ioannidis JP, Saltychev M, Most SP. The 10-item Standardized Cosmesis and Health Nasal Outcomes Survey (SCHNOS) for functional and cosmetic rhinoplasty. *JAMA Facial Plast Surg*. 2018;20(1):37–42.
21. Sicard RM, Shah R, Frank-Ito DO. Analyses on the influence of normal nasal morphological variations on odorant transport to the olfactory cleft. *Inhal Toxicol*. 2022;34(11-12):350–358.
22. Shah R, Frank-Ito DO. The role of normal nasal morphological variations from race and gender differences on respiratory physiology. *Respir Physiol Neurobiol*. 2022;297:103823.
23. Shah R, Marcus JR, Frank-Ito DO. Computational analysis of olfactory airspace in patients with unilateral cleft lip nasal deformity. *Cleft Palate Craniofac J*. 2021;58(10):1242–1250.
24. Frank-Ito DO, Carpenter DJ, Cheng T, et al. Computational analysis of the mature unilateral cleft lip nasal deformity on nasal patency. *Plast Reconstr Surg Global Open*. 2019;7(5):e2244.
25. Marcus JR, Brown DA, Carpenter D, Glener A, Allori A, Frank-Ito D. Multimodal characterization of the mature septal deformity and airspace associated with unilateral cleft lip and palate. *Plast Reconstr Surg*. 2019;143(3):865–873.
26. Patki A, Frank-Ito DO. Characterizing human nasal airflow physiologic variables by nasal index. *Respir Physiol Neurobiol*. 2016;232:66–74.
27. Sicard RM, Frank-Ito DO. Role of nasal vestibule morphological variations on olfactory airflow dynamics. *Clin Biomech (Bristol, Avon)*. 2021;82:105282.
28. Leopold DA, Hummel T, Schwob JE, Hong SC, Knecht M, Kobal G. Anterior distribution of human olfactory epithelium. *Laryngoscope*. 2000;110(3 Pt 1):417–421.
29. Holbrook EH, Wu E, Curry WT, Lin DT, Schwob JE. Immunohistochemical characterization of human olfactory tissue. *Laryngoscope*. 2011;121(8):1687–1701.
30. Soler ZM, Pallanch JF, Sansoni ER, et al. Volumetric computed tomography analysis of the olfactory cleft in patients with chronic rhinosinusitis. *Int Forum Allergy Rhinol*. 2015;5(9):846–854.
31. Borojeni AAT, Garcia GJM, Moghaddam MG, et al. Normative ranges of nasal airflow variables in healthy adults. *Int J Comput Assist Radiol Surg*. 2020;15(1):87–98.
32. Kimbell JS, Frank DO, Laud P, Garcia GJ, Rhee JS. Changes in nasal airflow and heat transfer correlate with symptom improvement after surgery for nasal obstruction. *J Biomech*. 18 2013;46(15):2634–2643.
33. Garcia GJ, Schroeter JD, Segal RA, Stanek J, Foureman GL, Kimbell JS. Dosimetry of nasal uptake of water-soluble and reactive gases: a first study of interhuman variability. *Inhal Toxicol*. 2009;21(7):607–618.
34. Doty RL. Olfactory dysfunction and its measurement in the clinic. *World J Otorhinolaryngol Head Neck Surg*. 2015;1(1):28–33.

35. Doty RL, Shaman P, Dann M. Development of the University of Pennsylvania Smell Identification Test: a standardized microencapsulated test of olfactory function. *Physiol Behav*. 1984;32(3):489–502.
36. Doty RL, Shaman P, Kimmelman CP, Dann MS. University of Pennsylvania Smell Identification Test: a rapid quantitative olfactory function test for the clinic. *Laryngoscope*. 1984;94(2 Pt 1):176–178.
37. Oliva AD, Gupta R, Issa K, et al. Aging-related olfactory loss is associated with olfactory stem cell transcriptional alterations in humans. *J Clin Invest*. 2022;132(4):e155506.
38. Nagase YN, N; Kato, T; Hayakawa, T. Epidemiological analysis of cleft lip and/or palate by cleft pattern. *J Maxillofac Oral Surg*. 2011;9(4): 389–395.
39. Lipan MM, Most SP. Development of a severity classification system for subjective nasal obstruction. *JAMA Facial Plast Surg*. 2013;15(5): 358–361.
40. Patel PN, Wadhwa H, Okland T, Kandathil CK, Most SP. Comparison of the distribution of standardized cosmesis and health nasal outcomes survey scores between symptomatic and asymptomatic patients. *Facial Plast Surg Aesthet Med*. 2022;24(4):305–309.
41. Doty R. Measurement of chemosensory function. *World J Otorhinolaryngol Head Neck Surg*. 2018;4:11–28.
42. Mani M, Morén S, Thorvardsson O, Jakobsson O, Skoog V, Holmström M. EDITOR'S CHOICE: objective assessment of the nasal airway in unilateral cleft lip and palate—a long-term study. *Cleft Palate Craniofac J*. 2010;47(3):217–224.
43. Sobol DL, Allori AC, Carlson AR, et al. Nasal airway dysfunction in children with cleft lip and cleft palate: results of a cross-sectional population-based study, with anatomical and surgical considerations. *Plast Reconstr Surg*. 2016;138(6):1275–1285.
44. Zhang RS, Lin LO, Hoppe IC, et al. Nasal obstruction in children with cleft lip and palate: results of a cross-sectional study utilizing the NOSE Scale. *Cleft Palate Craniofac J*. 2019;56(2):177–186.
45. Fernandes MBL, Salgueiro AGNS, Bighetti EJB, Trindade-Suedam IK, Trindade IEK. Symptoms of obstructive sleep apnea, nasal obstruction, and enuresis in children with nonsyndromic cleft lip and palate: a prevalence study. *Cleft Palate Craniofac J*. 2019;56(3):307–313.
46. Shih CS, Sykes JM. Correction of the cleft-lip nasal deformity. *Facial Plast Surg*. 2002;18(4):253–262.
47. Friel MT, Starbuck JM, Ghoneima AM, et al. Airway obstruction and the unilateral cleft lip and palate deformity: contributions by the bony septum. *Ann Plast Surg*. 2015;75(1):37–43.
48. Fitzek M, Patel PK, Solomon PD, et al. Integrated age-related immunohistological changes occur in human olfactory epithelium and olfactory bulb. *J Comp Neurol*. 2022;530(12):2154–2175.
49. Durante MA, Kurtenbach S, Sargi ZB, et al. Single-cell analysis of olfactory neurogenesis and differentiation in adult humans. *Nat Neurosci*. 2020;23(3):323–326.
50. Ramprasad VH, Frank-Ito DO. A computational analysis of nasal vestibule morphologic variabilities on nasal function. *J Biomech*. 2016;49(3):450–457.
51. Dong J, Ma J, Shang Y, et al. Detailed nanoparticle exposure analysis among human nasal cavities with distinct vestibule phenotypes. *J Aerosol Sci*. 2018;121:54–65.
52. Inthavong K, Ma J, Shang Y, et al. Geometry and airflow dynamics analysis in the nasal cavity during inhalation. *Clin Biomech*. 2019;66:97–106.
53. Ma J, Dong J, Shang Y, Inthavong K, Tu J, Frank-Ito DO. Air conditioning analysis among human nasal passages with anterior anatomical variations. *Med Eng Phys*. 2018;57:19–28.
54. Nishijima H, Kondo K, Yamamoto T, et al. Influence of the location of nasal polyps on olfactory airflow and olfaction. *Int Forum Allergy Rhinol*. 2018;8(6):695–706.
55. Alam S, Li C, Bradburn KH, Zhao K, Lee TS. Impact of middle turbinectomy on airflow to the olfactory cleft: a computational fluid dynamics study. *Am J Rhinol Allergy*. 2019;33(3):263–268.